Supplemental Material

Online Figure I

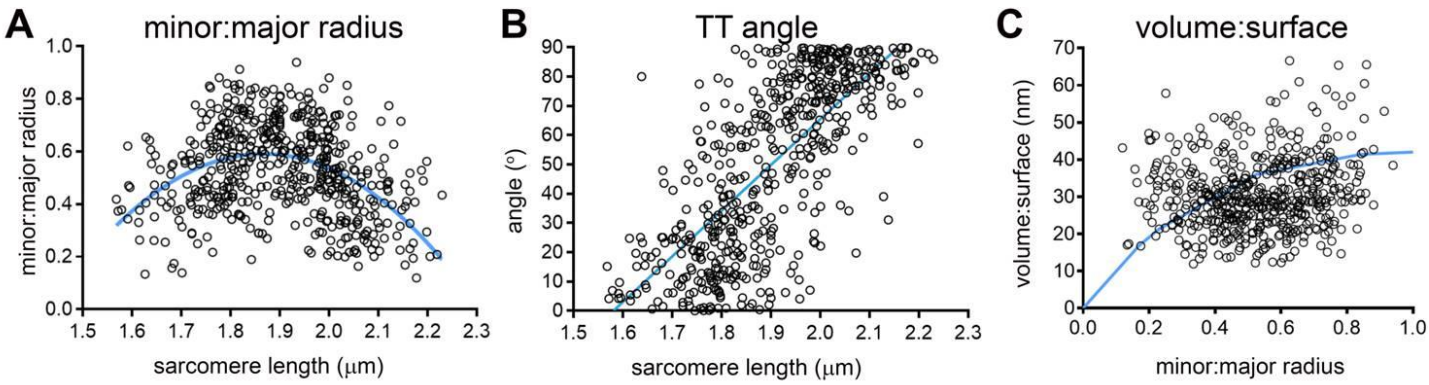

Online Figure I. Supplementary information on TT shape and orientation during static changes in SL (chemically fixed whole hearts). A: *TT cross-section minor:major radius ratio at different SL. Data was assessed using non-linear quadratic fit (blue curve). Statistical significance was assessed comparing a mixed effects model to a constant model; p<0.0001.* ***B:*** *Minimum angle between major axis of TT cross-sections and Z-disc. Statistical significance was assessed using a linear regression fit comparing a mixed effects model to a constant model; p<0.0001.* ***D:*** *Volume:surface ratio of TT segments at different TT cross-section minor:major radius ratios. Data fitted with a realistic geometric shape-based model. Statistical significance was assessed using a mixed effects model to a constant model; assessed using cubic fit (not shown), p<0.0001. N = 7 hearts/ 29 tissue samples/ 125 cells/ 539 TT (see also Online Table I). P-values indicate whether a fitted model is more suitable than assuming a constant relationship.*

Online Figure II

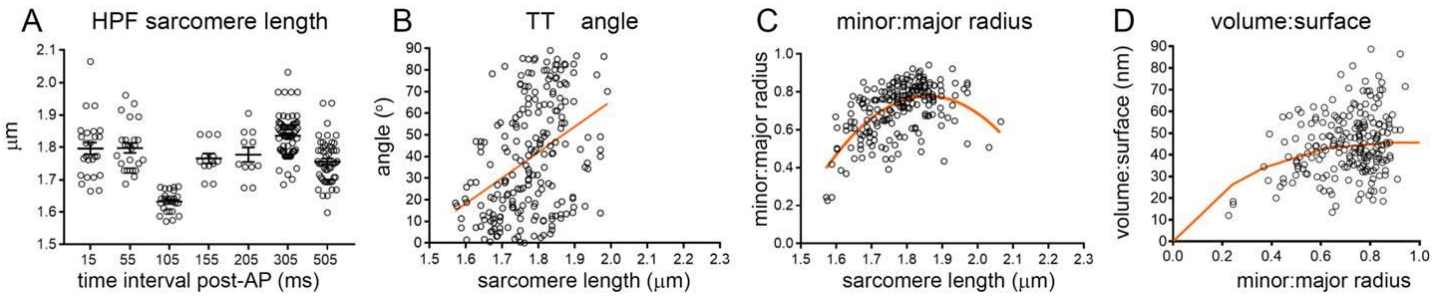

Online Figure II. Supplementary information on TT shape and orientation of TT during dynamic changes in SL (HPF-preserved contracting cells). ***A:*** *SL in cardiomyocytes, HPF-preserved with different lag-times after the last (tenth) electrical stimulus, showing that peak contraction of cells in the HPF chamber is reached at ~105 ms post-stimulation, followed by relaxation.* ***B:*** *Minimum angle between major axis of TT cross-section and Z-disc. Statistical significance was assessed using a linear regression fit (orange line) comparing a mixed effects model to a constant model; p<0.0001.* ***C:*** *TT cross-section minor:major radius ratio at different SL. Data was assessed using non-linear quadratic fit (orange curve). Statistical significance was assessed comparing a mixed effects model to a constant model; p<0.0001.* ***D:*** *Volume:surface ratio of TT segments at different TT cross-section minor:major radius ratios. Data fitted with a realistic geometric shape-based model. Statistical significance was assessed using a mixed effects model to a constant model; assessed using linear fit (not shown); p<0.001. N = 2 hearts/ 16 tissue samples/ 56 cells/ 214 TT (see also Online Table II). P-values indicate whether a fitted model is more suitable than assuming a constant relationship.*

Online Figure III

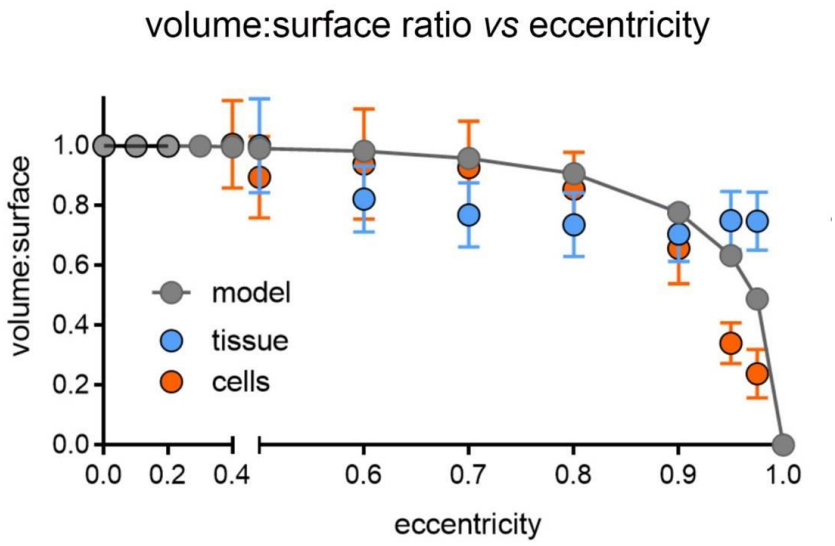

Online Figure III. Relationship between TT volume:surface ratio and eccentricity in tissue, cells, and predicted behaviour when modelling elliptical TT with constant circumference. *Blue dots: tissue data; orange dots: cell data; grey dots and line: model data.*

Online Figure IV

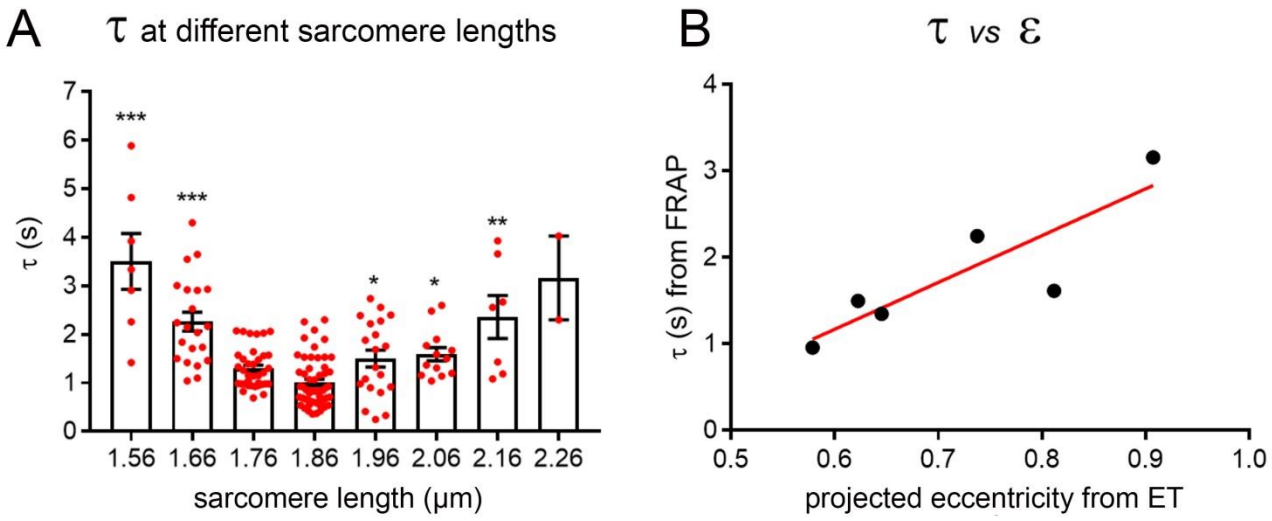

Online Figure IV. A: Fluorescence recovery times as a function of SL / TT eccentricity during static deformation (live cell experiments). A: *FRAP time constant* t *during static cell deformation is lowest in cells at rest (SL 1.86 ± 0.1 μm), and it increases with the extent of both contracture and stretch. Data was binned (bin size 0.1 μm) and analysed using Kruskal-Wallis test with Dunn's post-hoc test (multiple comparisons vs 1.86 μm), *p<0.05, **p<0.01, ***p<0.001, N = 7 hearts/ 89 cells.* ***B:*** *Relationship between average* t *and eccentricity, projected from SL in ET cell data.*

Online Figure V

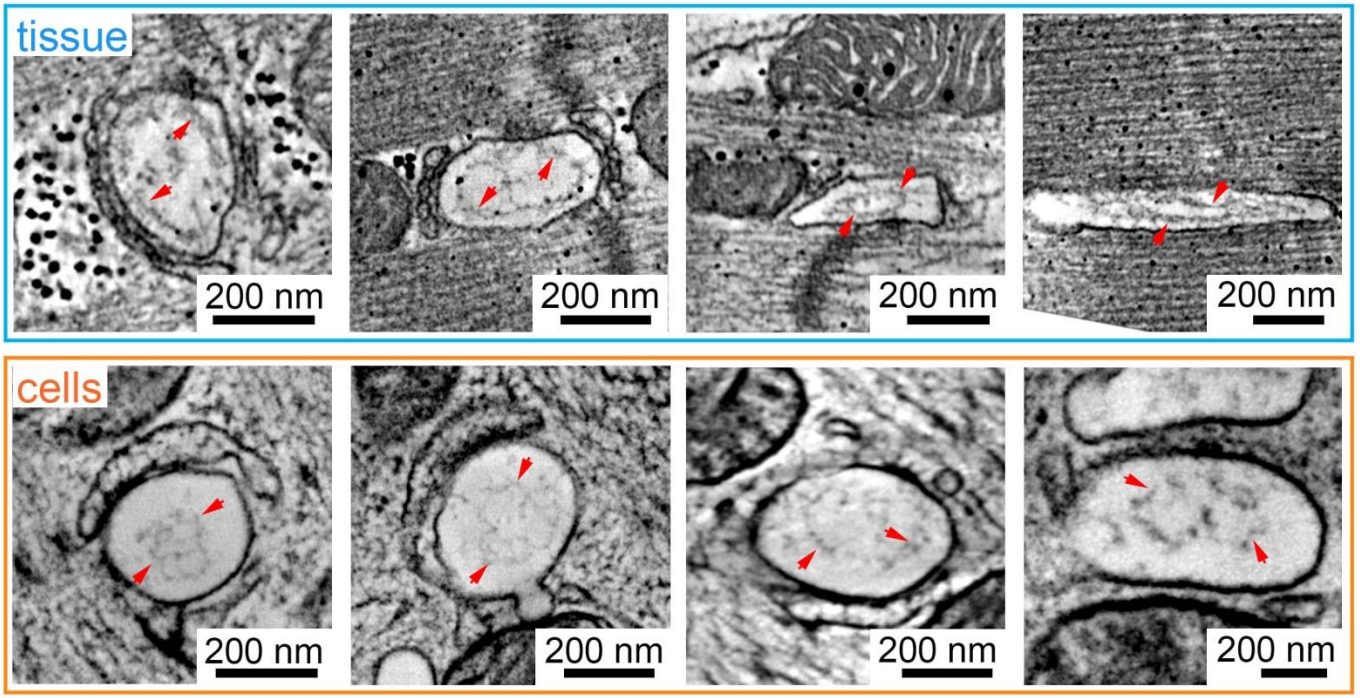

Online Figure V. Representative images of TT glycocalyx in chemically fixed tissue and high-pressure frozen cells. *Representative ET slices demonstrating the presence of a glycocalyx (basal lamina) layer in TT of different eccentricities in tissue (blue, top) and isolated cells (bottom, orange). Red arrows indicate the glycocalyx.*

Online Figure VI

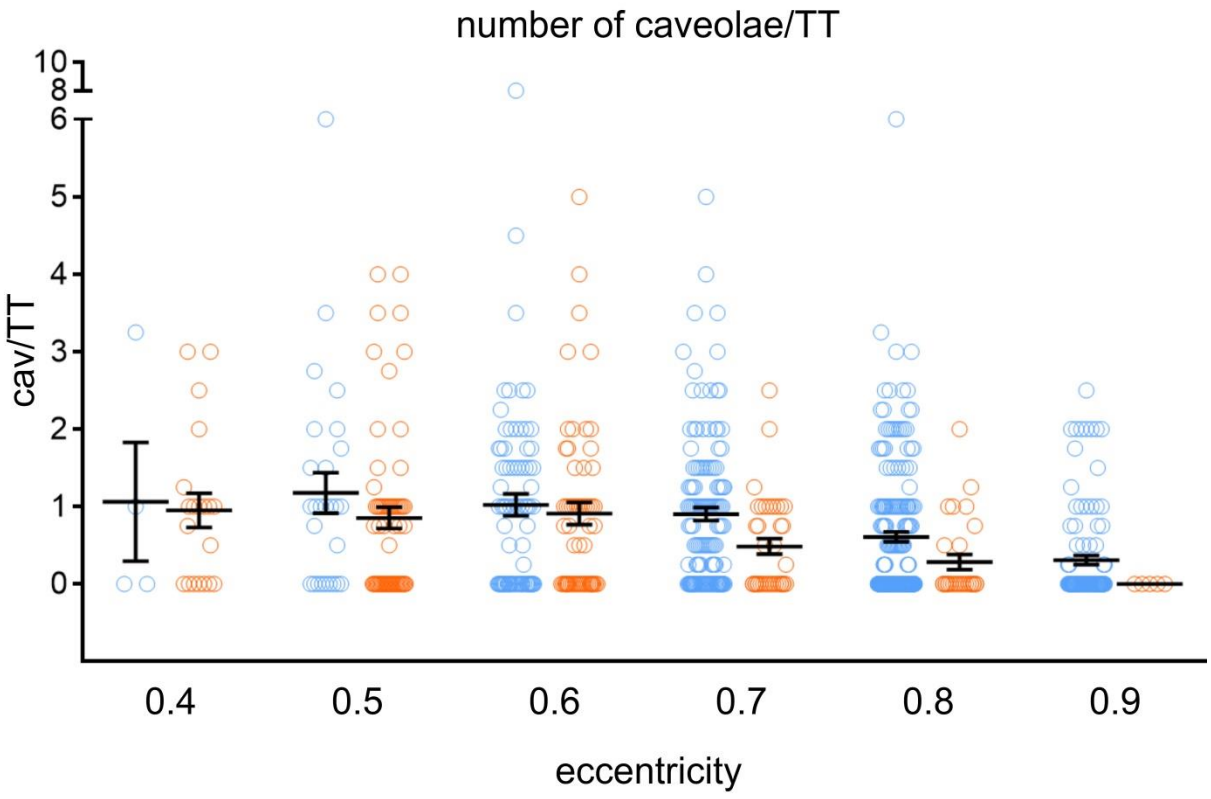

Online Figure VI. Presence of caveolae is inversely related to TT eccentricity during static (chemically fixed tissue) and dynamic (HPF-preserved cells) mechanical deformation. *Number of caveolae per 250 nm-long TT segment as a function of TT eccentricity. Binned values, bin size 0.1, pooled data across all the hearts (blue) / cells (orange). Data was assessed using a Kruskal-Wallis test, p<0.5 for both tissue and cells. Tissue: N = 7 hearts/ 29 tissue samples/ 125 cells/ 539 TT (Online Table I); cells: N = 2 hearts/ 16 preparations/ 56 cells/ 214 TT (Online Table II).*

Online Figure VII

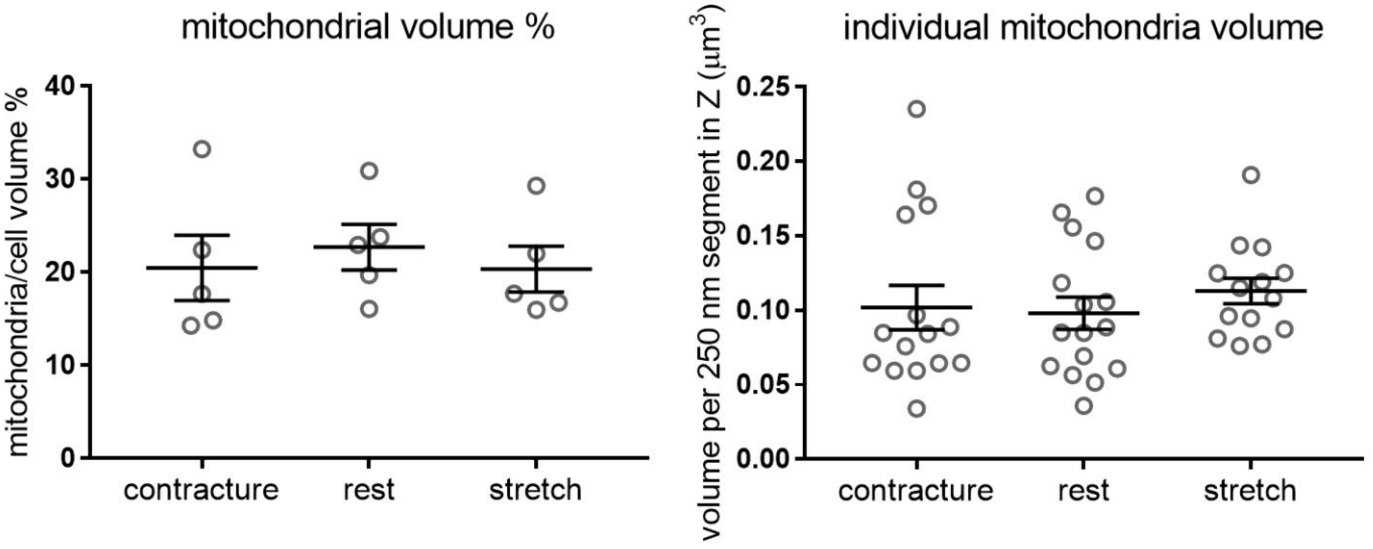

Online Figure VII. Lack of significant changes in mitochondrial volume between contracture, rest, and stretch (tissue data)*. Left: Partial mitochondrial volume per total cell volume in n = 5 representative electron tomographic volumes per mechanical state (each stack containing on average 8 mitochondria). Right: absolute volume of individual mitochondrial segments contained within these stacks (250 nm depth). Stacks representative of N = 2 or 3 hearts for contracture/stretch or rest, respectively. Data presented as mean±SEM, statistical significance assessed using Kruskal-Wallis test; p = 0.5672 (left), p = 0.659 (right).*

Online Figure VIII

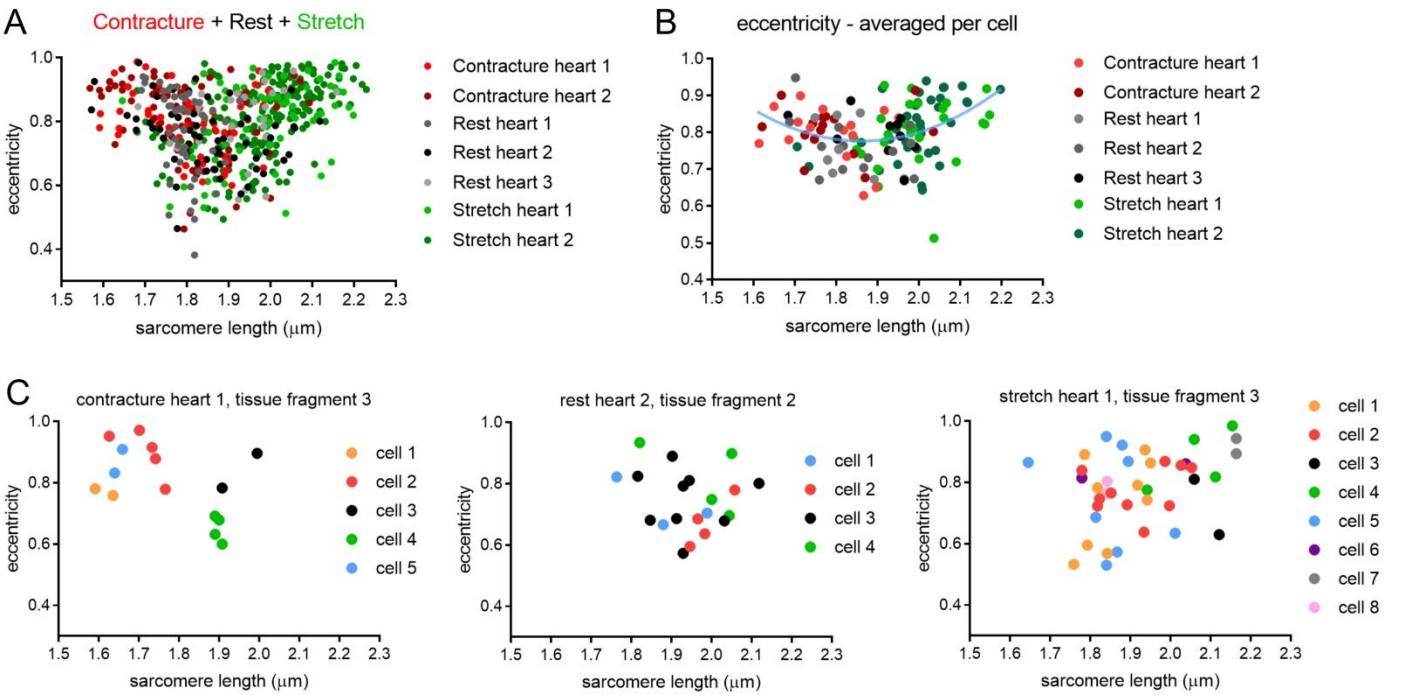

Online Figure VIII. Representative per-sample data distribution (here shown TT eccentricity in tissue) demonstrating the high degree of SL heterogeneity within individual samples, and the close relation of read-outs to SL length. A: *Distribution of individual data points across all 7 hearts studied (colour-coded, see also Online Table I).* ***B:*** *Data averaged per cell, statistical analysis was performed by comparing a mixed effects model to a constant model; quadratic fit, p<0.0001.* ***C:*** *Representative distribution of data points in individual tissue fragments obtained from hearts preserved in contracture (left), rest (middle), and stretch (right). Note the presence of heterogeneity of SL even within individual cells (colour-coded).*

Online Figure IX

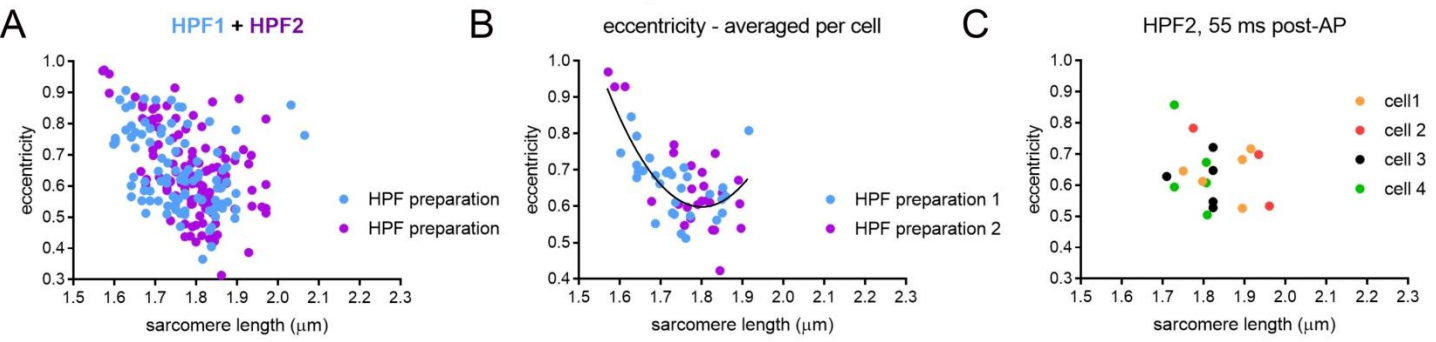

Online Figure IX. Representative per-sample data distribution (here shown TT eccentricity in cells) demonstrating the high degree of SL heterogeneity within individual samples, and the close relation of read-outs to SL length. A: *Distribution of individual data points across 2 high-pressure frozen (HPF) preparations.* ***B:*** *Data averaged per cell, statistical analysis was performed by comparing a mixed effects model to a constant model; quadratic fit, $p<0.0001$.* ***C:*** *Representative data distribution within one experimental group. Note the presence of heterogeneity of SL even within individual cells (colour-coded).*

Online Table I and II

Online Table I. Tissue data distribution across individual hearts. Stated are the number of tissue fragments, cells, and individual TT analysed, as well as the prescribed mechanical state: contracture, rest, and stretch.

	Heart 1	Heart 2	Heart 3	Heart 4	Heart 5	Heart 6	Heart 7
Mechanical state prescribed	Contracture	Contracture	Rest	Rest	Rest	Stretch	Stretch
Tissue fragments	4	5	3	2	4	5	8
Cells	15	15	8	14	10	26	37
TT	51	73	53	62	28	84	188
Summary	9 tissue fragments 30 cells 124 TT		9 tissue fragments 32 cells 143 TT			11 tissue fragments 63 cells 272 TT	

Online Table II. Cell data distribution across individual hearts. Stated are the number of cells and individual TT analysed per each heart/time post-AP interval.

	Post-AP (ms)	cells	TT	Summary
Heart 1	15	7	15	30 cells, 96 TT
	55	3	7	
	105	8	17	
	155	4	7	
	205	2	6	
	305	4	33	
	505	2	11	
Heart 2	15	4	10	26 cells, 118 TT
	55	4	18	
	105	4	7	
	155	1	5	
	205	2	5	
	305	4	32	
	505	7	41	

Online Table III

Online Table III. Details of statistical analyses. *1| - indicates random effect. Except for 4B, Online IVA, Online VI, Online VII, the coef test within Matlab was used. This is a test which returns the p-value for an F-test with the hypothesis that all fixed-effects coefficients except for the intercept are 0.*

Figure	Exact p-value	Estimate of Fit	Mixed effects - equation
1C, Online IB	6.25×10^{-70}	$-239.81 + 152.32 \times SL$	angle = 1 + SL + (1| heart) + (1| fragment) + (1| cell)
1D	1.86×10^{-20}	$8.1173 + (-7.832) \times SL + 2.083 \times SL^2$	eccentricity = 1 + SL + SL^2 +(1| heart) + (1| fragment) + (1| cell)
1E	8.35×10^{-11}	$88.964 + (-132.63) \times$ eccentricity $+ 74.575 \times$ eccentricity^2	volumetosurface = 1 + eccentricity + eccentricity^2 +(1| heart) + (1| fragment) + (1| cell)
2C, Online IB	9.27×10^{-11}	$-200.54 + 135.63 \times SL$	angle = 1 + SL + (1| heart) + (1| cell)
2D	3.74×10^{-17}	$14.656 + (-15.129) \times SL + 4.0664 \times SL^2$	eccentricity = 1 + SL + SL^2 +(1| heart) + (1| cell)
2E	3.12×10^{-2}	$54.55 + (-15.604) \times$ eccentricity	volumetosurface = 1 + eccentricity +(1| heart) + (1| cell)
3C	1.76×10^{-20}	$151.37 + (-210.35) \times SL + 96.068 \times SL^2 + (-14.193) \times SL^3$	tau = 1 + SL + SL^2 + SL^3 + (1| heart) + (1| cell)
4B	2.5×10^{-3}	-	-
Online IA	8.49×10^{-25}	$-11.034 + 12.399 \times SL + (-3.3038) \times SL^2$	mintomajorradius = 1 + SL + SL^2 +(1| heart) + (1| fragment)) + (1| cell)
Online IC	4.35×10^{-10}	$39.815 + (-47.003) \times$ mintomajorradius $+ 53.942 \times$ mintomajorradius^2	volumetosurface = 1 + mintomajorradius + mintomajorradius^2 +(1| heart) + (1| fragment)) + (1| cell)
Online IIC	6.37×10^{-22}	$-15.28 + 17.253 \times SL + (-4.6329) \times SL^2$	mintomajorradius = 1 + SL + SL^2 +(1| heart) + (1| cell)
Online IID	3.74×10^{-4}	$26.811 + 25.072 \times$ mintomajorradius	volumetosurface = 1 + mintomajorradius +(1| heart) + (1| cell)
Online IVA	7.64×10^{-11}	multiple comparisons *vs* 1.86 µm; *vs* $1.56 - 5.36 \times 10^{-6}$, *vs* $1.66 - 2.86 \times 10^{-8}$, *vs* $1.96 - 4.66 \times 10^{-2}$, *vs* $2.06 - 9.6 \times 10^{-3}$, *vs* $2.16 - 2.28 \times 10^{-3}$	
Online VI	4.29×10^{-9}; 4.1×10^{-3}	tissue; cells respectively	
Online VII	5.67×10^{-1}, 6.59×10^{-1}	left; right, respectively	